

MAGNETOCALORIC EFFECTS OF BARIUM-STRONTIUM FERRITES FOR MAGNETIC REFRIGERATION SYSTEM

Ummay HABIBA¹, Sheikh Manjura HOQUE², Samia Islam LIBA², Hasan Khaled ROUF^{1,*}

¹Department of Electrical & Electronic Engineering, University of Chittagong, Chittagong – 4331, Bangladesh
²Material Science Division, Bangladesh Atomic Energy Centre, Ramna, Dhaka, Bangladesh

Abstract

A study of the magnetocaloric effect (MCE) of Barium-Strontium-Ferrites $BaO \cdot SrO \cdot xFe_2O_3$ and $BaO \cdot SrO \cdot xFe_3O_4$ ($x=5.6, 5.8, 6$) is reported in this article. Using hematite of analytical grade and magnetite from Cox's Bazar beach sand mineral as ferrite contents, the hexaferrites were synthesized and their magnetic properties and MCE were systematically studied. The results indicate that the samples are strongly ferromagnetic and have high Curie temperature. All the samples are of second-ordered phase and exhibit large magnetic entropy changes. Among all the samples $BaO \cdot SrO \cdot 5.8Fe_2O_3$ and $BaO \cdot SrO \cdot 5.8Fe_3O_4$ exhibit the maximum entropy changes at the temperatures near and below the Curie temperature.

Keywords: magnetocaloric effects, hexaferrites, ferromagnetism, magnetic entropy.

Introduction

In recent years a lot of research is going on toward the development of economical, durable and dependable cooling system both from the materials science as well as engineering viewpoints. Conventional refrigeration systems use harmful gases such as chlorofluorocarbons (CFCs) and hydro-chlorofluorocarbons (HCFCs) as coolant materials which are detrimental to the Ozone layer of the atmosphere. In the evolution of cooling techniques energy-efficient and environment-friendly magnetic refrigeration can be a promising alternative to the conventional vapour-compression refrigeration techniques. Magnetic refrigeration is based on the magnetocaloric effect (MCE) [1-2] and can be used in residential cooling, space science, medical applications etc. as well as to cool down computer microchip ICs with the use of microfluidic channels.

MCE is a magneto-thermodynamic phenomenon which refers to the cooling or heating of a magnetic material by exposing the material to a changing magnetic field. When exposed to a changing magnetic field, suitable materials undergo magnetic entropy as well as temperature changes [3]. At a temperature near the Curie point, a ferromagnetic material tends to become paramagnetic material and spins of the material become random. Upon the application of an external magnetic field, spins tend to become parallel to the applied magnetic field. If the system is adiabatic, the internal energy of the system decreases, and it creates a cooling effect [4]. Some rare earth metals and their alloys are ideal for producing the largest temperature change, although, the major concern is the cost.

Magnetic refrigeration technology has been applied both at low and high temperatures. Materials used for magnetic refrigeration at low temperatures are mainly paramagnetic salts [5] but there are some drawbacks of using such salt materials. Since these materials are hydrated in order to avoid dehydration they need to be encapsulated in a hermetic container. The main requirement for magnetic refrigeration materials is to get large magnetic entropy change which

can be obtained when the material has large Curie temperature. The challenges for the application of MCE for magnetic refrigeration at high temperature include reducing the requirement of applied magnetic fields and enhancing the magnetic refrigeration efficiency [5].

Most of the materials working at low temperatures cannot be directly utilized for magnetic refrigeration. This is because to ensure refrigeration efficiency the heat transferred by each magnetizing-demagnetizing cycle of the refrigerator should be considerably large since the heat capacity near the ambient temperature is significantly increased. Therefore, new materials with large entropy change around the ambient temperature need to be studied [6]. Initially a large MCE of Gd ($T_C=293$ K) was observed in 1968 [7]. However, the entropy changes of some other magnetocaloric materials reported subsequently are much smaller than that of Gd. The entropy change of $Gd_5Si_2Ge_2$ with a first order phase transition is ~ 18 J/kgK around $T_C = 278$ K for a field change of 0–5 T, which is significantly larger than that of Gd (~ 10 J/kgK) under a similar condition [8]. $La_{1-x}Ca_xMnO_3$ ($x = 0.2$) has a large entropy change of 5.5 J/kgK at 230 K for a field change of 0–1.5 T [9]. Some new magnetocaloric materials with a first-order magnetic transition such as $LaFe_{13-x}Si_x \cdot MnAs_{1-x}Sb_x$, and $MnFeP_{0.45}As_{0.55}$ were found to have entropy changes from 18 J/kgK to 30 J/kgK [6,10-11].

Studies of magnetocaloric properties of different kinds of magnetocaloric materials such as ferromagnetic perovskites, glass ceramics, oxide-based composites, spinel ferrites etc. have been performed in many recent works [12]. Magnetocaloric effects in a nickel ferrite nanoparticle system and nickel-zinc ferrite nanoparticles were studied in [13] and [14], respectively. It is observed that while the MCE is not as large as that reported in bulk systems but ferrite nanoparticles have the advantages of being easily produced. In these cases the magnetocaloric properties strongly depend on the particle size which can be considered as a key tuning parameter in the optimization of magnetic refrigeration. A comparative study of the magnetocaloric effect of two different types of chemically synthesized magnetic nanoparticle systems, namely, cobalt ferrite and manganese zinc ferrite is reported in [15]. It is shown that the change in entropy with the change in applied magnetic field is reasonably large for this class of nanoparticles and has a wide distribution over a broad temperature range covering the region above and below the blocking temperature. Also the maximum entropy change is influenced by the particle size, overall distribution in anisotropy and magnetic moments. The effect of zinc substitution on the magnetic and magnetocaloric properties of $Cu_{1-x}Zn_xFe_2O_4$ ($x=0.6, 0.7, 0.8$) ferrites over a wide temperature range has been investigated in [16].

In this work, we have successfully synthesized the $BaO \cdot SrO \cdot xFe_2O_3$ and $BaO \cdot SrO \cdot xFe_3O_4$ ($x= 5.6, 5.8, 6$) hexaferrites by solid-state method using hematite of analytical grade and magnetite from Cox's Bazar beach sand mineral as ferrite contents. The magnetic properties and MCE in the intermetallic compounds were systematically studied. The results show that the samples are strong ferromagnetic materials and have high Curie temperature. All the samples are of second ordered phase and exhibits large magnetic entropy changes. Among all the samples $BaO \cdot SrO \cdot 5.8Fe_2O_3$ and $BaO \cdot SrO \cdot 5.8Fe_3O_4$ exhibit the maximum entropy changes at the temperatures near and below the Curie temperature and are promising candidates for magnetic refrigeration.

Experimental Procedure

Sample preparation technique is a vital part for ferrites processing which is explained in [17]. Here we used the solid state reaction method involving milling of reactions followed by sintering. $BaO \cdot SrO \cdot xFe_2O_3$ ($x=5.6, 5.8, 6$) were prepared from $BaCO_3 \cdot SrCO_3$ and hematite while $BaCO_3 \cdot SrCO_3$ and magnetite were used to prepare $BaO \cdot SrO \cdot xFe_3O_4$ ($x=5.6, 5.8, 6$). Agate mortar (hand milled) was used for intimate mixing of the materials for 4 hours for fine homogeneous mixing. Then the pre-sintering process was applied to the mixed samples at a

temperature between 850 °C to 900 °C for 5 hours to form ferrite through chemical reaction. The pre-sintered materials were milled for another 4 hours in distilled water to reduce them to small crystallites of uniform size. The mixtures were then dried, and polyvinyl alcohol was added as a binder. The formed powders were pressed under a pressure of 15-20 KN.cm⁻² in a stainless-steel die to make pellets, rods and toroids. Then the resulting pressed pellet, rod and toroid shaped samples were sintered at 1250 °C temperature for 4 hours and then cooled in the furnace. The phase pure characteristics of the samples were confirmed by the XRD patterns.

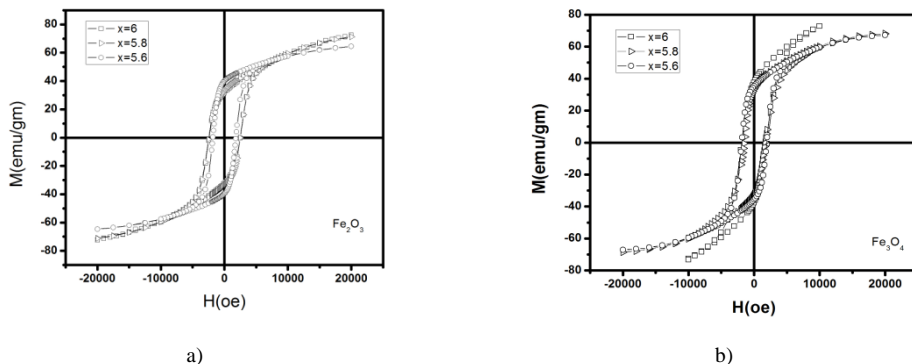


Fig. 1. Hysteresis loops of (a) BaO•SrO•xFe₂O₃ for x=5.6, 5.8, 6 and (b) BaO•SrO•xFe₃O₄ for x=5.6, 5.8, 6

Results and Discussions

Magnetic Properties

Magnetic properties of BaO•SrO•xFe₂O₃ and BaO•SrO•xFe₃O₄ (x= 5.6, 5.8, 6) were shown in our previous work [17]. The hysteresis loops for Ba-Sr-ferrites using hematite and magnetite and magnetite are shown in Fig. 1 while the variations of magnetic fields at different temperatures for all samples are given in Fig. 2. From these plots, we determined the Curie temperature of the samples. To determine the Curie temperature more precisely we also observed the dM/dT versus T curves for all the samples which are shown in Fig. 3.

Table 1 summarizes the magnetic parameters of the samples obtained from the Vibrating Sample Magnetometer. All the samples have very high coercive fields (H_c), remanent magnetizations (M_r), saturation magnetization (M_s) confirming their strong ferromagnetic nature. For both Ba-Sr-ferrites saturation magnetization decreases with the decrease of ferrite content concentration. Ferrites using hematite have higher Curie temperatures than those prepared using magnetite. These results manifest that BaO•SrO•xFe₂O₃ is more ferromagnetic than BaO•SrO•xFe₃O₄.

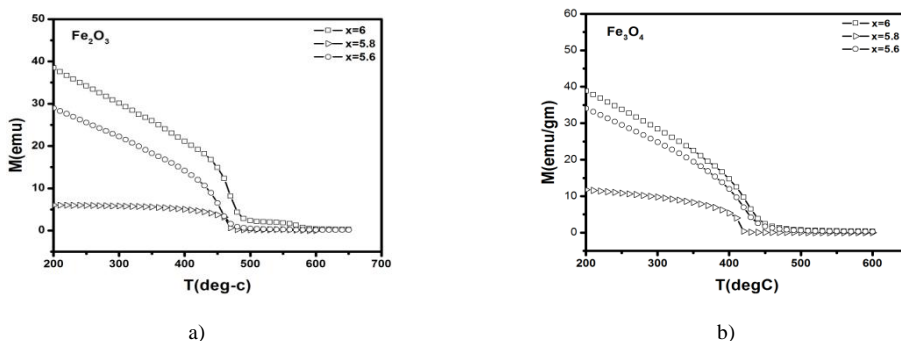


Fig. 2. M-T curves for (a) BaO•SrO•xFe₂O₃ with x=5.6, 5.8, 6 and (b) BaO•SrO•xFe₃O₄ with x=5.6, 5.8, 6

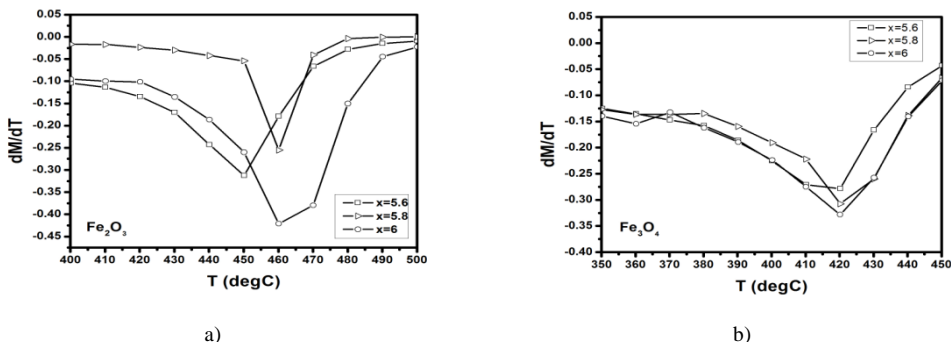


Fig. 3. $dM/dT - T$ curves for (a) $BaO \cdot SrO \cdot xFe_2O_3$ with $x=5.6, 5.8, 6$ and (b) $BaO \cdot SrO \cdot xFe_3O_4$ with $x=5.6, 5.8, 6$

Table 1. Saturation magnetization (M_s), remanent magnetization (M_r), coercive field (H_c) for all samples

| | X | H_c (oe) | M_r (emu) | M_s (emu) |
|-----------|-----|------------|-------------|-------------|
| Fe_2O_3 | 6 | 2468.15 | 3.18E+01 | 7.25E+01 |
| | 5.8 | 2476.096 | 3.35E+01 | 7.13E+01 |
| | 5.6 | 1810.477 | 3.98E+01 | 6.46E+01 |
| Fe_3O_4 | 6 | 1897.688 | 3.55E+01 | 7.31E+01 |
| | 5.8 | 1931.297 | 3.76E+01 | 6.84E+01 |
| | 5.6 | 1588.256 | 3.31E+01 | 6.72E+01 |

Magnetocaloric Properties

The magnetocaloric behavior of the samples is studied by observing the magnetic entropy change ΔS with temperature. The temperature regions, where the samples display a transition from a ferromagnetic to a paramagnetic state are observed carefully. The change in entropy was calculated using the thermodynamic Maxwell relation from the family of M-H curves taken at different temperatures. In such magnetic or magneto-structural transitions, the corresponding Arrott plot (square of the magnetization against H/M ratio) is drawn. The areas under the curves for the magnetization at different temperature are measured and are plotted for each sample. Fig. 4 shows the isothermal magnetization curves for $BaO \cdot SrO \cdot xFe_2O_3$ and $BaO \cdot SrO \cdot xFe_3O_4$ ($x= 5.6, 5.8, 6$) samples while the areas under these isothermal curves for the same samples at various temperatures are shown in Fig. 5. For each sample, among the isothermal curves, a large gap between two curves is obtained around the temperature at which magnetic entropy change due to magnetocaloric effect is maximum. On the other hand, samples which show first-order phase transition exhibit a negative slope [4].

Fig 6. shows the Arrott plots of $BaO \cdot SrO \cdot xFe_2O_3$ and $BaO \cdot SrO \cdot xFe_3O_4$ ($x= 5.6, 5.8, 6$) from which it is observed that slopes of all the six samples are positive indicating second-order phase transitions. The T_c estimated from the M–T curve and from the Arrott plots are close to each other Fig 7 and Fig. 8 plots the temperature dependence of magnetic entropy change (ΔS) for all the samples over a wide temperature range around their respective T_c . A broad maximum of ΔS around their respective T_c are observed for all curves. As the ferrite content increases, the magnitude of ΔS increases under a given field strength. The Curie temperature, maximum entropy change and temperature for maximum entropy change for all the samples are given in the Table 2.

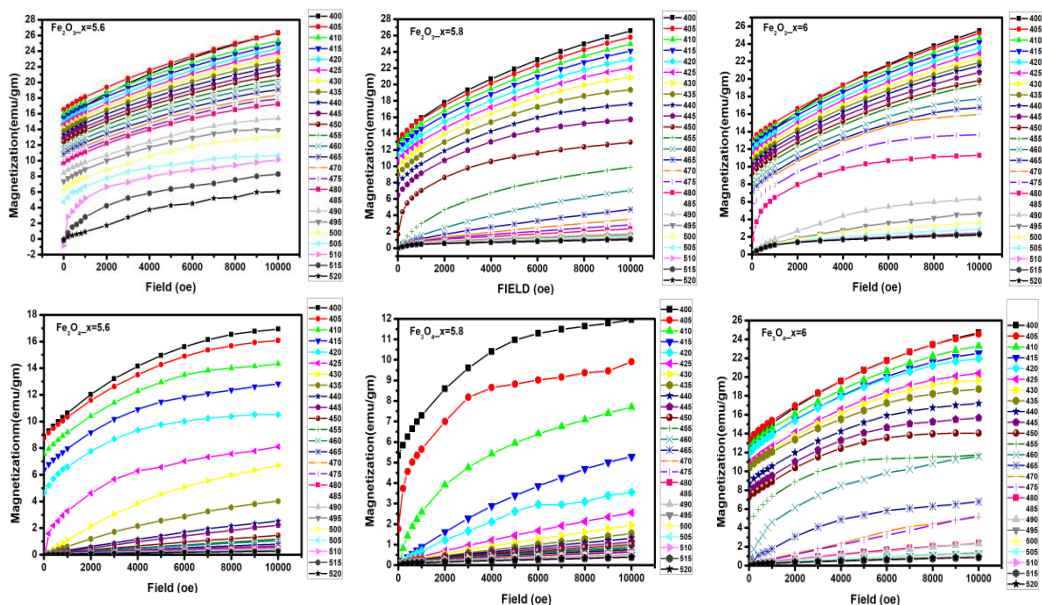


Fig. 4. Isothermal magnetization curves at different temperature for $\text{BaO}\cdot\text{SrO}\cdot x\text{Fe}_2\text{O}_3$ $x= (5.6, 5.8, 6)$ (upper) and $\text{BaO}\cdot\text{SrO}\cdot x\text{Fe}_3\text{O}_4$ ($x=5.6, 5.8, x=6$) (lower)

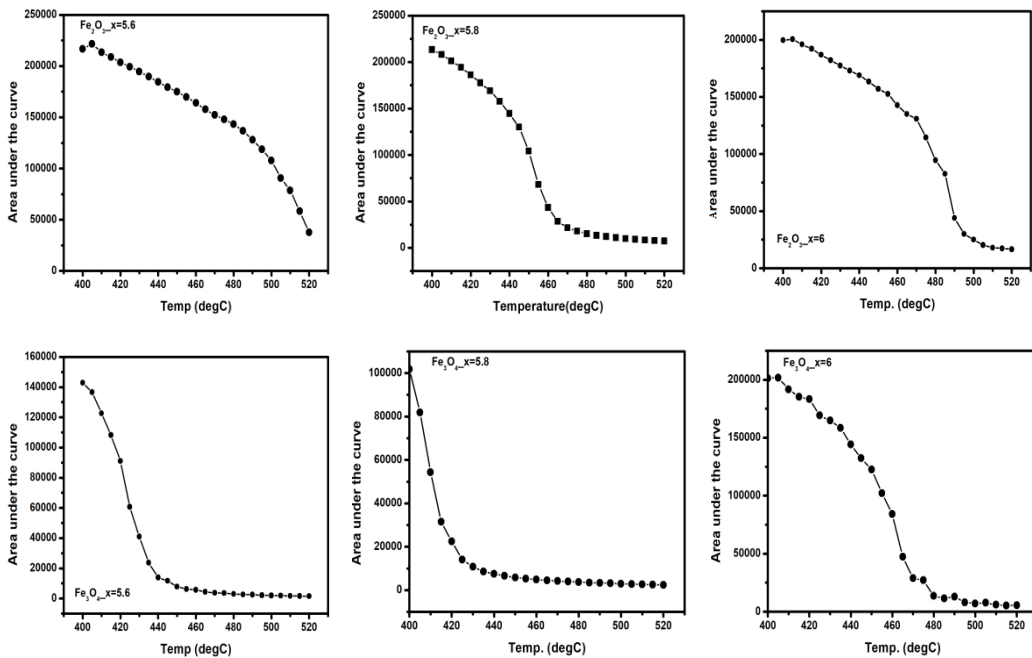


Fig. 5. Area under the isothermal curve at various temperatures for $\text{BaO}\cdot\text{SrO}\cdot x\text{Fe}_2\text{O}_3$ $x= (5.6, 5.8, 6)$ (upper) and $\text{BaO}\cdot\text{SrO}\cdot x\text{Fe}_3\text{O}_4$ ($x=5.6, 5.8, x=6$) (lower)

Table 2. Curie temperature, maximum entropy change and temperature for maximum entropy change for the samples

| Samples | T _c (°C) | Max. entropy change (J/kg/°C) | Temp. for max. entropy change (°C) |
|---|---------------------|-------------------------------|------------------------------------|
| BaO•SrO•5.6Fe ₂ O ₃ | 450 | 4.25 | 520 |
| BaO•SrO•5.8Fe ₂ O ₃ | 460 | 7.5 | 455 |
| BaO•SrO•6Fe ₂ O ₃ | 460 | 8 | 490 |
| BaO•SrO•5.6Fe ₃ O ₄ | 420 | 6 | 425 |
| BaO•SrO•5.8Fe ₃ O ₄ | 420 | 5.5 | 410 |
| BaO•SrO•6Fe ₃ O ₄ | 420 | 7.5 | 465 |

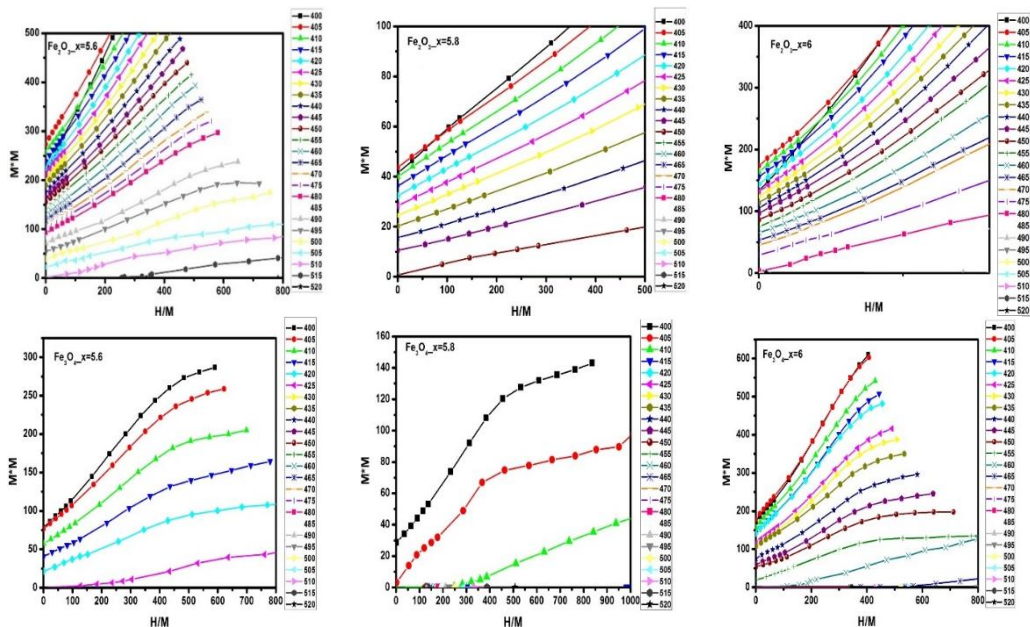


Fig. 6. Arrot plots for BaO•SrO•xFe₂O₃ x= (5.6, 5.8, 6) (upper) and BaO•SrO•xFe₃O₄ (x=5.6, 5.8, x=6) (lower)

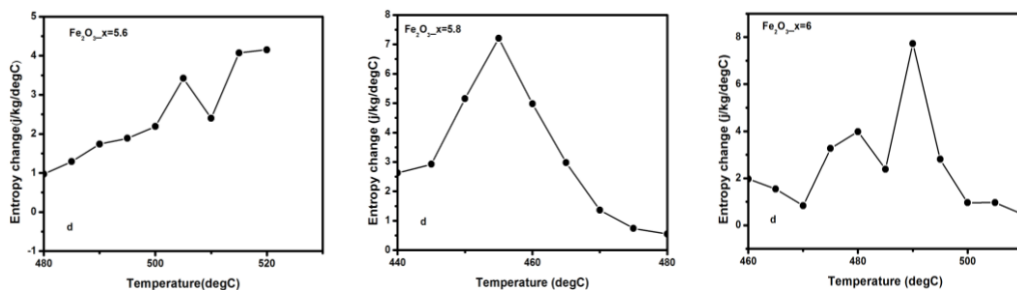


Fig. 7. Temperature dependence magnetic entropy change (ΔS) for BaO•SrO•xFe₂O₃ x= (5.6, 5.8, 6)

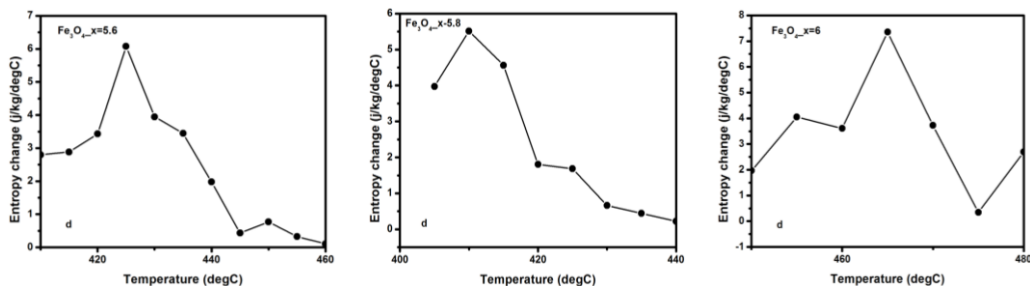


Fig. 8. Temperature dependence magnetic entropy change (ΔS) for $\text{BaO}\cdot\text{SrO}\cdot x\text{Fe}_3\text{O}_4$ ($x=5.6, 5.8, 6$)

It is observed that among the samples, $\text{BaO}\cdot\text{SrO}\cdot 5.8\text{Fe}_2\text{O}_3$ and $\text{BaO}\cdot\text{SrO}\cdot 5.8\text{Fe}_3\text{O}_4$ exhibit the maximum entropy changes at the temperatures near / below the Curie temperature. For $\text{BaO}\cdot\text{SrO}\cdot 5.8\text{Fe}_2\text{O}_3$ the maximum entropy change is at 455°C (below the Curie temperatures 460°C) and for $\text{BaO}\cdot\text{SrO}\cdot 5.8\text{Fe}_3\text{O}_4$ it is at 410°C (below the Curie temperatures 420°C). In other cases the maximum entropy change occurs at a temperature higher than the Curie temperature. Therefore, $\text{BaO}\cdot\text{SrO}\cdot 5.8\text{Fe}_2\text{O}_3$ and $\text{BaO}\cdot\text{SrO}\cdot 5.8\text{Fe}_3\text{O}_4$ exhibit better magnetocaloric effects than other four. Because of the demonstrated magnetocaloric effects, these two samples can be promising for use in magnetic refrigeration.

Conclusion

Magnetic and magnetocaloric properties of $\text{BaO}\cdot\text{SrO}\cdot x\text{Fe}_2\text{O}_3$ and $\text{BaO}\cdot\text{SrO}\cdot x\text{Fe}_3\text{O}_4$ ($x=5.6, 5.8, 6$) which were prepared using hematite of analytical grade and magnetite from Cox's bazaar beach sand mineral were studied in this work. The hysteresis loops for Ba-Sr-ferrites indicate that the samples are of ferromagnetic type. The Curie temperatures for ferrites using hematite are higher than those using magnetite. The results indicate that all the samples are of second ordered phase and exhibit large magnetic entropy changes. Among all the samples $\text{BaO}\cdot\text{SrO}\cdot 5.8\text{Fe}_2\text{O}_3$ and $\text{BaO}\cdot\text{SrO}\cdot 5.8\text{Fe}_3\text{O}_4$ exhibit the maximum entropy changes at the temperatures near and below the Curie temperature and demonstrate potentials for magnetic refrigeration.

References

- [1] E. Warburg, *Magnetische Untersuchungen*, **Annalen der Physik**, 249(5), 1881, pp. 141-164.
- [2] W. F. Giauque and D. P. MacDougall, *Attainment of Temperatures Below 1° Absolute by Demagnetization of $\text{Gd}_2(\text{SO}_4)_3\cdot 8\text{H}_2\text{O}$* , **Physical Review**, 43(9), 1933, 768.
- [3] T. D. Thanh, N. H. Yen, N. H. Dan, T.-L. Phan, and S.-C. Yu, *Magnetic Properties and Large Magnetocaloric Effect in Amorphous Fe-Ag-Ni-Zr for Room-Temperature Magnetic Refrigeration*, **IEEE Transactions on Magnetics**, 51(1), 2015, pp. 1-4.
- [4] L. Li, *Review of Magnetic Properties and Magnetocaloric Effect in the Intermetallic Compounds of Rare Earth with Low Boiling Point Metal(s)*, **Chinese Physics B**, 10, 2015, pp. 1-56.
- [5] J. Du, Q. Zheng, Y. B. Li, Q. Zhang, D. Li, and Z. D. Zhang, *Large Magnetocaloric Effect and Enhanced Magnetic Refrigeration in Ternary Gd-based Bulk Metallic Glasses*, **Journal of Applied Physics**, 103, 2008, 023918.

-
- [6] B. G. Shen, J. R. Sun, F. X. Hu, H. W. Zhang, Z.H. Cheng, *Recent Progress in Exploring Magnetocaloric Materials*, **Advanced Materials**, 21(45), 2009, pp. 4545-4564.
- [7] G. V. Brown, *Magnetic Heat Pumping Near Room Temperature*, **Journal of Applied Physics**, 47, 1976, 3673.
- [8] V.K. Pecharsky and K.A. Gschneidner Jr., *Giant Magnetocaloric Effect in $Gd_5Si_2Ge_2$* , **Physical Review Letters**, 78, 1997, 4494.
- [9] Z. B. Guo, Y. W. Du, J. S. Zhu, H. Huang, W. P. Ding, and D. Feng, *Large Magnetic Entropy Change in Perovskite-Type Manganese Oxides*, **Physical Review Letters**, 78, 1997, 1142.
- [10] H. Wada and Y. Tanabe, *Giant magnetocaloric effect of $MnAs_{1-x}Sb_x$* , **Applied Physics Letters**, 79, 2001, 3302.
- [11] O Tegus, E. Brück, K. H. J. Buschow, F. R. de Boer, *Transition-metal-based Magnetic Refrigerants for Room-Temperature Applications*, **Nature**, 415, 2002, pp. 150–152.
- [12] N. R. Ram, M. Prakash, U. Naresh, *Review on Magnetocaloric Effect and Materials*, **Journal of Superconductivity and Novel Magnetism**, 31(7), 2018, pp. 1971–1979.
- [13] J. Gass, N. Frey, M. Morales, et al., *Magnetic Anisotropy and Magnetocaloric Effect (MCE) in $NiFe_2O_4$ Nanoparticles*. **MRS Proceedings**, 962, 2006, 0962-P05-03.
- [14] K. D. Lee, R. C. Kambale, N. Hur, *Magnetocaloric effect in Ni-Zn ferrite nanoparticles prepared by using solution combustion*, **Journal of the Korean Physical Society**, 65(11), 2014, pp. 1930–1934.
- [15] P. Poddar, J. Gass, J. Rebar, *Magnetocaloric effect in ferrite nanoparticles*, **Journal of Magnetism and Magnetic Materials**, 307, 2006, pp. 227-231.
- [16] S. Akhter, D. P. Paul, S. M. Hoque, M. A. Hakim, M. Hud, R. Mathieu, P. Nordblad, *Magnetic and Magnetocaloric Properties of $Cu_{1-x}Zn_xFe_2O_4$ ($x = 0.6, 0.7, 0.8$) Ferrites*, **Journal of Magnetism and Magnetic Materials**, 367, 2014, pp. 75 – 80.
- [17] U. Habiba, H. K. Rouf and S. M. Hoque, *Structural and Magnetic Characterizations of Barium-Strontium-Ferrites using Hematite of Analytical Grade and Magnetite from Cox's Bazar Beach Sand Mineral*, **European Journal of Materials Science and Engineering**, 2(2-3), 2017, pp. 41-50.
-

Received: November 16, 2018

Accepted: December 04, 2018